MDPI

Article

Delimitation of Urban Hot Spots and Rural Cold Air Formation Areas for Nocturnal Ventilation Studies Using Urban Climate Simulations

Florian Steigerwald [1,2], Meinolf Kossmann [1,*], Heike Schau-Noppel [1], Saskia Buchholz [1] and Oleg Panferov [2]

1 Deutscher Wetterdienst, 63067 Offenbach, Germany
2 TH Bingen–University of Applied Sciences, 55411 Bingen am Rhein, Germany
* Correspondence: meinolf.kossmann@dwd.de; Tel.: +49-69-8062-2969

Abstract: Due to global warming, the conservation or enhancement of urban ventilation during synoptically calm and hot weather conditions is receiving increasing attention in climate resilient urban and regional planning. The transport of cool air from rural surroundings into the city by local winds during nighttime is important for the alleviation of the urban heat island intensity and heat load in particular. A simple statistical method, which objectively identifies urban thermal hot spots and areas of rural cold air formation from thermodynamic urban climate model simulations is described and applied to Aschaffenburg, a medium-sized town located in hilly terrain in south-central Germany. The delimited hot spots and nocturnal cold air formation areas are influenced by local land cover, and also by the surrounding landscape heterogeneity, surface energy exchange and atmospheric mixing processes. The results illustrate limitations of hot spot or cool spot estimation methods based purely on the analysis of classified land cover data. Nocturnal backward airflow trajectories from thermal hot spots in the city and forward trajectories from rural areas with substantial cold air formation are calculated to determine which cold air formation areas are contributing to ventilation and advective cooling of thermal hot spots. It is found that nocturnal ventilation mechanisms are not bound to municipal boundaries, which highlights the need for regional cooperation in urban climate adaptation. The described method provides guidance to urban and regional planners in order to protect important cold air formation areas, e.g., from urban sprawl, and it can be applied to study impacts of planning scenarios. Options for improvement or extension of the method are discussed.

Keywords: urban heat islands; urban planning; drainage winds; country breeze; z-transformation; airflow trajectories

1. Introduction

Summer heat load conditions in cities are enhanced by the urban heat island (UHI) phenomenon and are becoming more intense and more frequent due to global warming [1–3]. Airflow from cooler rural surroundings into a city is an important cooling process to reduce heat load for urban dwellers (Figure 1). Under synoptic scale calm and clear weather conditions, local wind systems such as country breezes and nocturnal drainage winds are the main mechanisms for ventilating cities with cool rural air [4–9]. Country breezes and drainage winds (down-slope and down-valley winds) are driven by air temperature differences between rural and urban areas, or between slopes or valleys and the air over adjacent plains [10,11].

The preservation or enhancement of: (1) nocturnal cold air formation in the rural airsheds surrounding a city; and (2) urban ventilation paths with low aerodynamic roughness (and low emissions of heat or pollutants) to enable penetration of rural air into the city are important measures to ensure or enhance urban ventilation [12–14]. Urban climate maps illustrating climate functions and sensitivities are a common tool to ensure consideration of urban ventilation in the process of urban development [15,16]. The method of forward

directed airflow trajectories from rural cold air formation areas are very useful to identify those cold air formation areas (CAs), which are relevant for ventilating a city, while backward directed airflow trajectories from thermal hot spots (THs) provide information about the source areas of the air reaching hot urban quarters [9,17,18].
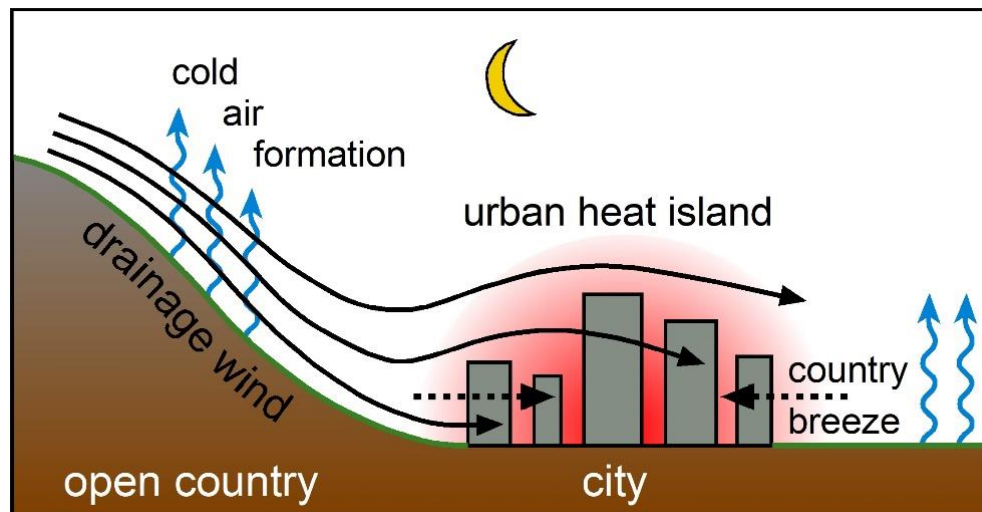

Figure 1. Schematic figure of a city located on a valley floor with illustrations of the urban heat island (red color shading), rural cold air formation (blue wavy arrows) and cold air flows by drainage winds (solid black arrows) and country breezes (dashed black arrows) during night time.

Traditionally, maps of THs and CAs are generated using climatopes [16,19]. Climatopes are defined as areas with similar microclimatic characteristics, such as the diurnal cycle of air temperature, surface roughness, land cover, topographic setting and exposure [19]. For simplicity, the spatial variations in microclimatic conditions were usually approximated by land cover classes and subjective interpretation of terrain height variability. Examples of commonly defined climatopes are: city-center climatope; commercial/industrial area climatope; park climatope; open country climatope; and water body climatope [20]. This qualitative approach of climatope definitions can be enhanced by quantitative analysis of satellite imagery, digital elevation models, 3-dimensional building datasets, vegetation indices, or surface heat budget simulations [21–23]. In recent years the classification of local climate zones (LCZs) has been introduced, which are now widely used in urban climate analyses [24,25]. LCZ definition is based on 3-dimensional building parameters, terrain roughness, pervious/impervious surface fractions, thermal surface conductivity, albedo and anthropogenic heat emissions. LCZs comprise of 10 built-up categories (e.g., compact high rise, open mid-rise, heavy industry, etc.) and seven categories without buildings (e.g., dense trees, low plants, water, etc.). Observations indicate a good correlation between air temperature and LCZs [26]. However, observations also demonstrate that thermal advection, variations in mixing height and terrain height or location within a city (e.g., downtown vs. urban fringe) cause substantial spatial variations in air temperatures within and between areas belonging to the same climatope or LCZ. Therefore, this contribution uses urban climate model results to identify THs and CAs in a physically based approach, as proposed in [26]. The cause and impact-based identification of THs and CAs enables more efficient and focused urban planning as well as more efficient climate change adaptation in urban areas.

This study applies a z-transformation [14,27] to identify and delimitate THs and CAs from thermodynamic urban climate model simulations for Aschaffenburg, a medium-sized city located in hilly terrain in south-central Germany. The applicability of this simple method for climate-resilient urban planning is further demonstrated using the simulated wind fields to calculate backward airflow trajectories from urban THs and forward trajectories from pronounced CAs in the rural vicinity to determine which CAs

are actually contributing to ventilation and advective cooling of THs and specific urban quartiers during nighttime in Aschaffenburg. This article is structured as follows: Chapter 2 introduces the study area, the urban climate simulations, the airflow trajectory calculation, and the z-transformation approach. Chapter 3 presents the results of the objectively identified THs and CAs, which are compared to the land cover classification used as input data for the numerical urban climate simulation. This is followed by the results of the nocturnal airflow trajectories starting from delimited THs and CAs. The main findings and limitations of the study and possibilities for improvement or extension of the presented approach are discussed in Chapter 4.

2. Methods

2.1. Study Area (Aschaffenburg)

The city of Aschaffenburg has a population of around 70,000 people and is located in the southeast of the Rhine–Main river plain in Germany, at the western edge of the low mountain range Spessart. As shown in Figures 2 and 3, the river Aschaff (name-giving to the city Aschaffenburg and Aschaff Valley) runs from northeast to southwest into the river Main. The city has an elevation of 133 m above sea level (asl) at its center and is flanked by mountain ridges exceeding 400 m asl in the north and the southeast. The mean air temperature at 2 m height in the period 1971–2000 as measured at the nearest weather station in Kahl am Main, is 10.2 °C [28]. This is 1.6 °C warmer than the corresponding spatially averaged mean air temperature in Germany. The higher temperature favors a higher risk of heat stress for the inhabitants, especially in the densely built-up city center [29,30]. Under synoptically calm and fair weather conditions, a thermally driven, diurnally oscillating valley wind system prevails in the Aschaff Valley (Figure 2b). Wind direction frequencies for daytime and nighttime hours in the warm season (April to September) are derived from a three-year wind dataset (30-min mean values) captured on top of a high building in the center of Aschaffenburg at 35 m above street level. Since Aschaffenburg is located at the exit of the Aschaff Valley, daytime up-valley winds blow from a relatively broad sector between southwest and west-northwest and nighttime down-valley winds blow from a smaller sector between northeast and east-northeast (Figure 2b).

2.2. Urban Climate Simulations (MUKLIMO_3, TRACA)

For modelling local climate conditions in the study area, the 3-dimensional microscale urban climate model MUKLIMO_3 is used in its thermodynamic version [31]. The model solves prognostic equations to simulate diurnal cycles of 3-dimensional fields of air temperature, humidity and wind [32], as well as balancing heat and moisture in the soil and it applies parameterizations of long-wave and short-wave radiation [33–35]. Plant canopy processes are simulated by a vegetation model for low plant canopies and trees [36]. In this study the meteorological effects of buildings are parameterized using gridded values of mean building height, building surface fraction and wall-area index (WAI = outer building wall areas per building surface area). For airflow simulations the urban canopy is treated as a porous medium [7]. The model does not include modules for simulating dynamic cloud or precipitation processes. The applicability of MUKLIMO_3 is therefore limited to dry weather conditions. In recent years MUKLIMO_3 has been applied to study the urban climate in various cities in central Europe [37–40].

In order to capture the meteorological effects of regional topography, a model domain of 40 km × 40 km centered on the city of Aschaffenburg is chosen (not shown). In the domain's central area of 18 km × 18 km (core area, Figure 2), the horizontal model grid resolution is set to 50 m. In the outer domain (outside the core area), the horizontal grid spacing is gradually stretched to 500 m. In the vertical direction model grid spacing is 10 m between 100 m asl (lowest point in the domain) to 250 m asl. Between 250 m and the top of the 3-dimensional model domain at 900 m asl, the vertical grid spacing is gradually stretched to 50 m. A 1-dimensional version of MUKLIMO_3 reaching up to 2500 m asl, with vertical grid spacing further stretched to 200 m at elevations above 900 m asl, is used to

provide model initialization values and boundary conditions at the top of the 3-dimensional model domain. The 12 km × 12 km modelling subdomain within the core area (Figure 2a) has been used for the presentation of results in all figures below.

The delimitations of THs and CAs, as well as airflow trajectory calculations presented in this study are based on a MUKLIMO_3 simulation for idealized calm and clear summer weather conditions. The 3-dimensional model simulation starts on the 17th of July at 08:00 CEST (Central European Summer Time) and ends on the 18th of July at 06:00 CEST. The water temperature of the rivers Main and Aschaff is set to 24 °C. A southerly airflow of 0.5 m/s at 200 m asl is prescribed for the initialization of the wind field calculation (using the 1-dimensional model).

The basic land cover model input is taken from the Copernicus Urban Atlas 2012 for the MUKLIMO_3 land cover classification (Figure 3) and from the Copernicus High Resolution Layer 2012 for the tree cover fraction and impervious surface area fraction [41,42]. Terrain elevation data and 3-dimensional building data (Level of Detail 1) for generating gridded data of mean building heights (Figure A1), building surface fraction (Figure A2), and WAI are taken from the German Federal Agency for Cartography and Geodesy [30,43].
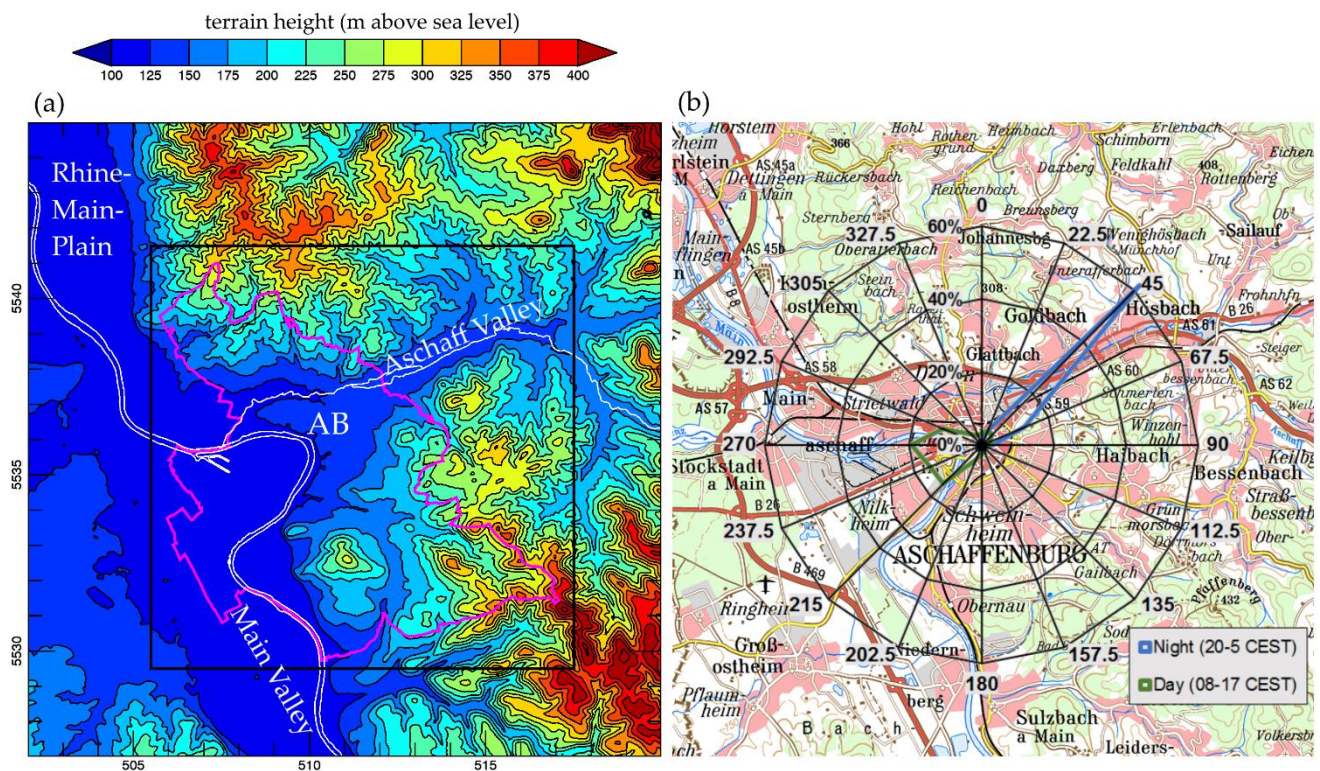

Figure 2. (**a**) Map of the terrain elevation in m asl in the 18 km × 18 km equidistant grid core area of the model domain. The 12 km × 12 km modelling subdomain for the presentation of results (black square), the city border (magenta contour), the city center (AB) of Aschaffenburg and the rivers Main and Aschaff (white contour) are also shown. (**b**) Topographic map of the 18 km × 18 km domain (reprinted with permission from [43]. 2009, GeoBasis-DE/BKG) with the wind rose observed under synoptically calm and fair weather conditions in the warm seasons (April–September), measured during the period of 2018–2020 on top of a high building in Aschaffenburg [43].
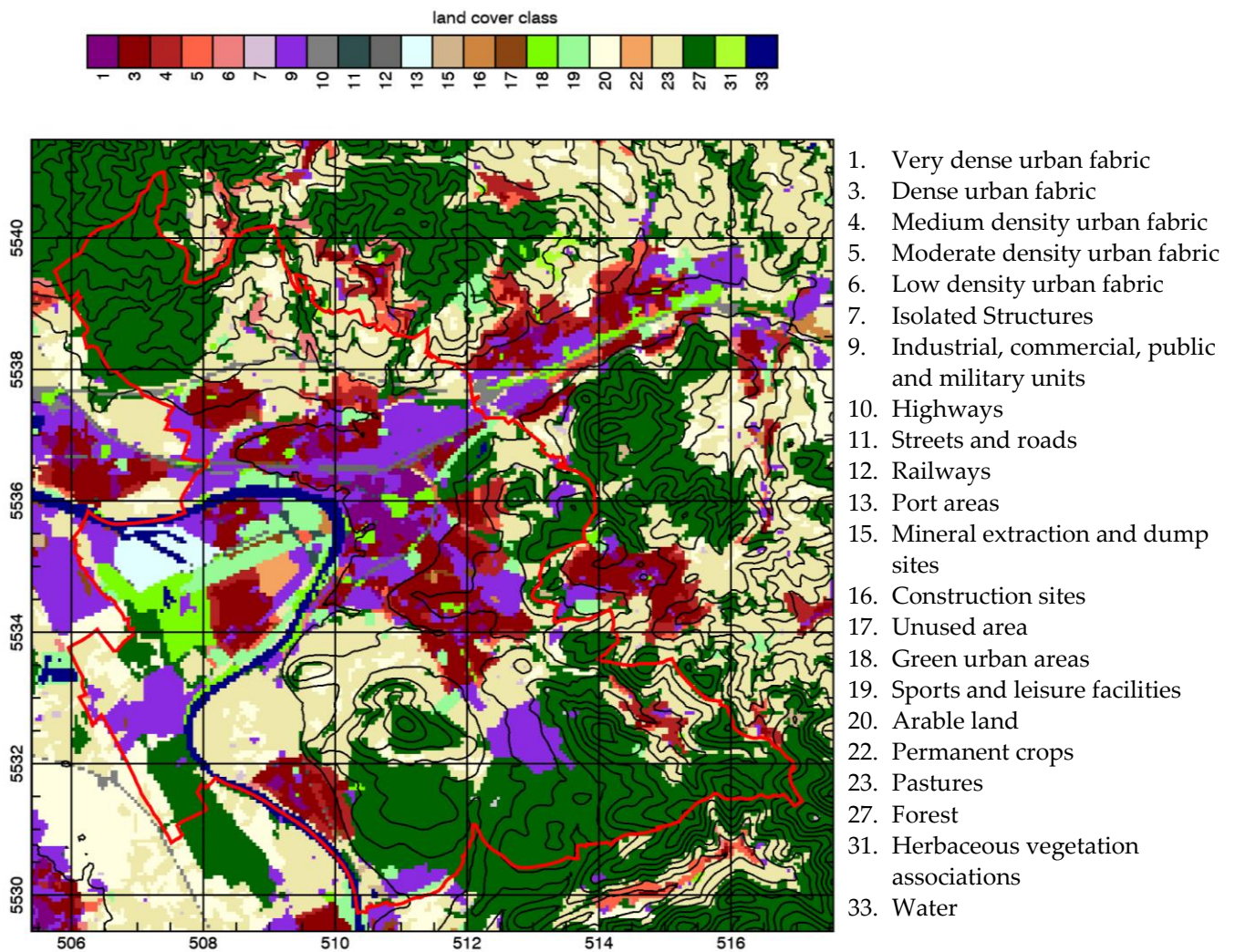
Figure 3. Land cover classification map in the 12 km × 12 km subdomain (see Figure 2a) with the city border of Aschaffenburg (red line). Black contour lines represent terrain elevation in 25 m height intervals.

Backward and forward airflow trajectories for studying ventilation in Aschaffenburg are derived in a post-processing procedure from 3-dimensional MUKLIMO_3 wind field output using the TRAjectory CAlculator (TRACA) [9,44]. TRACA randomly releases massless particles at domains such as CAs or THs and tracks their paths in the study area. TRACA needs coordinate polygon data to determine the release areas and information about the height above ground and timing of particle releases.

This study focuses on TH and CA delimitation for the analysis of nocturnal ventilation in Aschaffenburg. To illustrate results from the MUKLIMO_3 simulation during nighttime, Figures 4 and 5 show the near surface wind field and air temperature distribution at 00:00 and 02:00 CEST, respectively. The heat island in the city center is prominent at midnight, with air temperatures about 3 K higher than in the rural surroundings (Figure 4). Air temperatures are not only elevated in the city center, but also in other built-up districts around the center. The air temperature difference between the city and the surroundings leads to a pressure difference, which causes country breezes, i.e., compensatory winds from surrounding cool areas towards hot urban quarters. The superposition of the country breezes and cold air drainage from the surrounding hills represents the major nocturnal ventilation process for Aschaffenburg under high-pressure weather conditions. The converging transport of cool air into the city center alleviates heat load in the densely built-up districts.
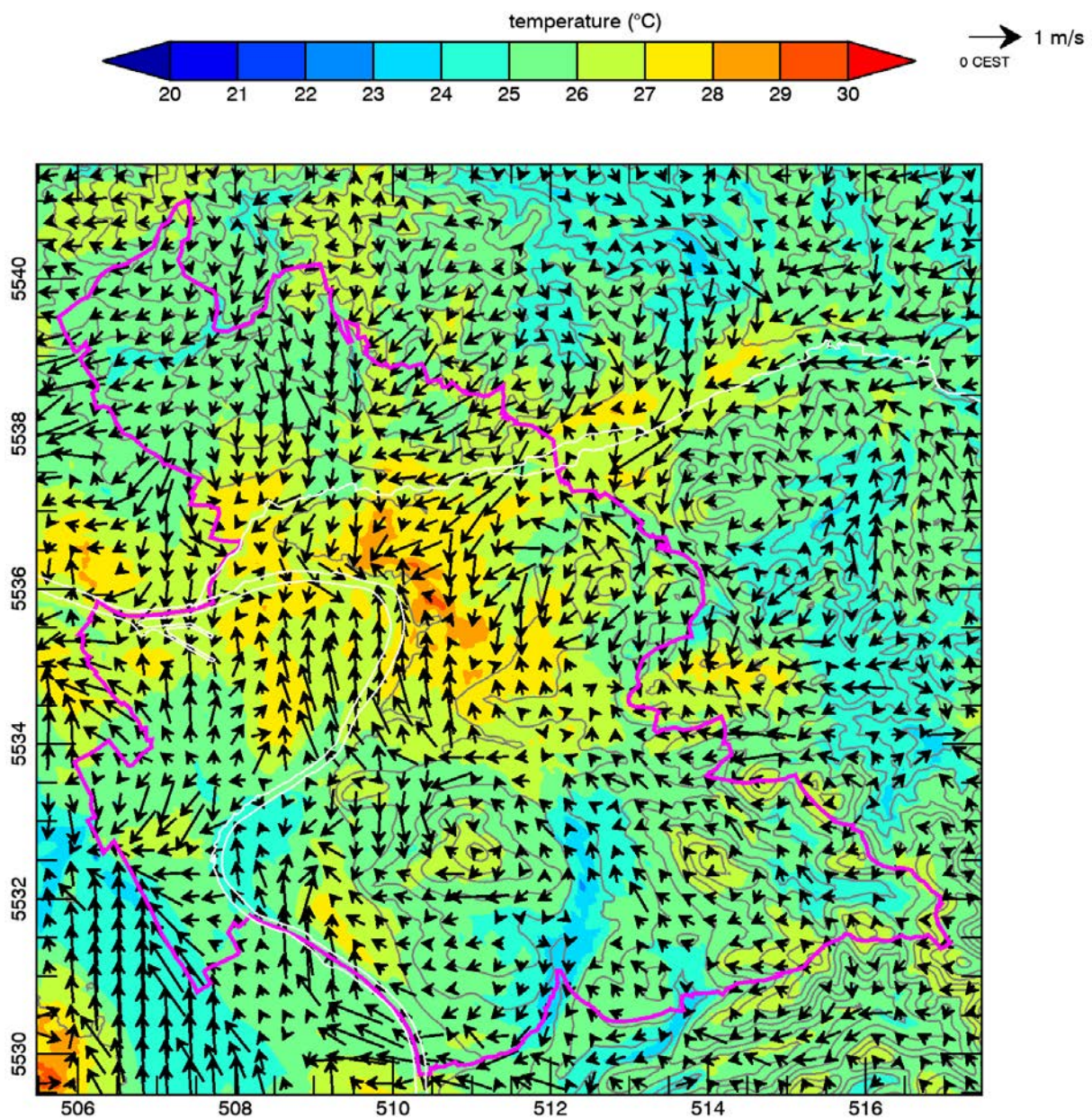
Figure 4. 00:00 CEST map of the air temperature (°C) and wind vectors (m/s) within the 12 km ×
12 km city subdomain at 5 m above ground level. Terrain elevation contour lines are shown in grey,
rivers in white, and the city border of Aschaffenburg in magenta.

At 02:00 CEST (Figure 5) the heat island intensity decreases to about 1–2 K, which
weakens the thermal forcing of country breezes and leads to a more developed mountain
wind in the Aschaff Valley. As a result of this, the surface wind field does not converge in
the city center anymore. Between 00:00 and 02:00 CEST cooling by about 3 K is simulated
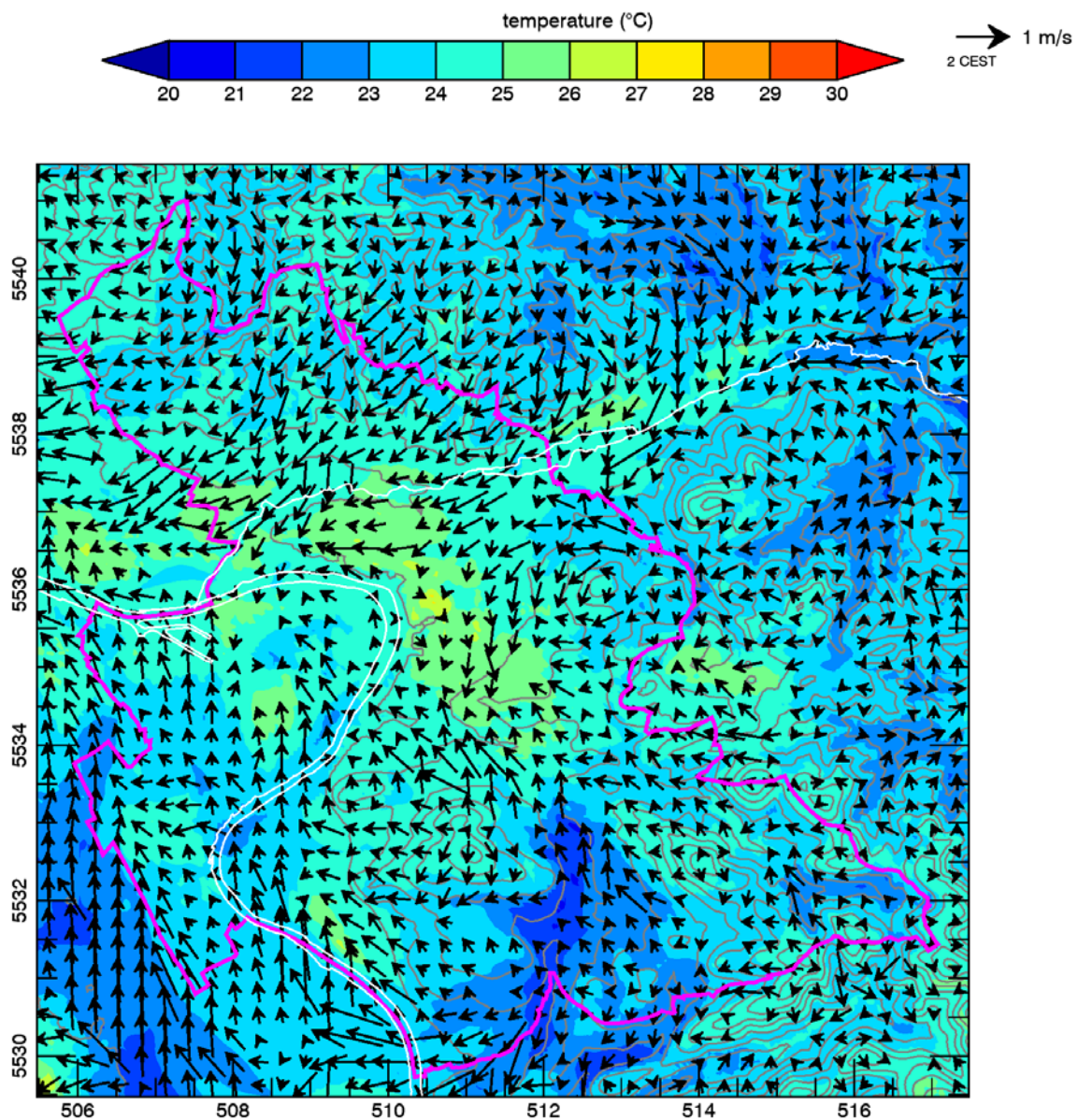in the city center.

Figure 5. 02:00 CEST map of the air temperature (°C) and wind vectors (m/s) within the 12 km × 12 km city subdomain at 5 m above ground level. Terrain elevation contour lines are shown in grey, rivers in white, and the city border of Aschaffenburg in magenta.

2.3. Objective Delimitation (z-Transformation)

The z-transformation approach (which is widely spread in geography [14,27]) is applied to quantitatively determine rural CAs and urban THs.

$$Z_{var}(x,y) = \frac{var(x,y) - \mu_{var}}{\sigma_{var}} \tag{1}$$

where Z_{var} at the location with spatial coordinates x and y is the normalized value of the variable var. μ_{var} and σ_{var} are the spatial mean value and standard deviation of var for a given domain and time, respectively [14,27]. For the delimitation of THs, the z-transformation is applied to the simulated variable (var) air temperature (T) at 5 m above ground level (agl) within the municipal boundaries of Aschaffenburg. A model grid cell belongs to a TH if its temperature value is higher than the spatial mean value for more than one standard deviation, i.e., $Z_T(x,y) > 1$.

For the delimitation of CAs, we apply the z-transformation to the variable (var) time-integrated sensible heat flux (H_{int}) between the ground and the atmosphere and between trees and the atmosphere from 22:00 to 04:00 CEST within the 12 km × 12 km city subdomain shown in Figures 3–5. Model grid cells with positive values of H_{int} (i.e., built-up areas with no cold air formation) are excluded from the CA analysis. Model grid cells belong to CAs if the value of H_{int} is lower than $\mu_{Hint} - 0.5\sigma_{Hint}$, i.e., lower than the mean value minus a half standard deviation ($Z_{Hint} < -0.5$).

The choice of the threshold values for THs and CAs identification (Z_T and Z_{Hint}) depends on the intended extremity of the variable used for delimitation and on the topography of the study area. For example, a study area with more pronounced relief would have stronger spatial variability in air temperature and therefore a higher σ_T value. For a city located at a valley bottom, a smaller threshold value Z_T might be applicable for TH delimitation. In order to avoid strongly pixelated THs and CAs, a spatial smoothing algorithm is applied to the gridded model MUKLIMO_3 output data of T and H_{int}, which is calculated as a moving average over one surrounding grid cell in each direction (average over 3 × 3 grid cells) for T, and two surrounding grid cells in each direction (5 × 5 grid cells) for H_{int}. While T is subject to atmospheric mixing processes, the stronger smoothing of H_{int} is used as it is influenced in a much stronger way by heterogenic local land cover. To provide climate information on the urban quarter scale, we are interested in the delimitation of well pronounced THs and CAs covering at least 50 connected model grid cells, which equals an area of 12.5 hectare (1 hectare = 10^4 m^2).

3. Results

3.1. Delimitated Thermal Hot Spots (20:00 CEST)

In order to determine the THs inside the city borders for nocturnal ventilation analysis, the simulated 20:00 CEST air temperature field in 5 m agl is chosen for z-transformation (Figure 6). At 20:00 CEST differential cooling between urban and rural areas already generates a well-developed UHI associated with multiple THs in the city center and surrounding built-up areas. Furthermore, at 20:00 CEST UHI structure and TH occurrence is still undisturbed by drainage winds, which become evident from about 22:00 CEST onwards. Figure 6 shows the objectively delimitated THs in a red outline. While most city districts and the city center with its air temperature still exceeding 32 °C are clearly visible, not all built-up areas within the city border are marked as THs due to their topographic location near areas with lower temperatures. In addition, the results show that larger parks and graveyards in the city are excluded from THs as a result of their lower air temperatures (Figures 3 and 6).
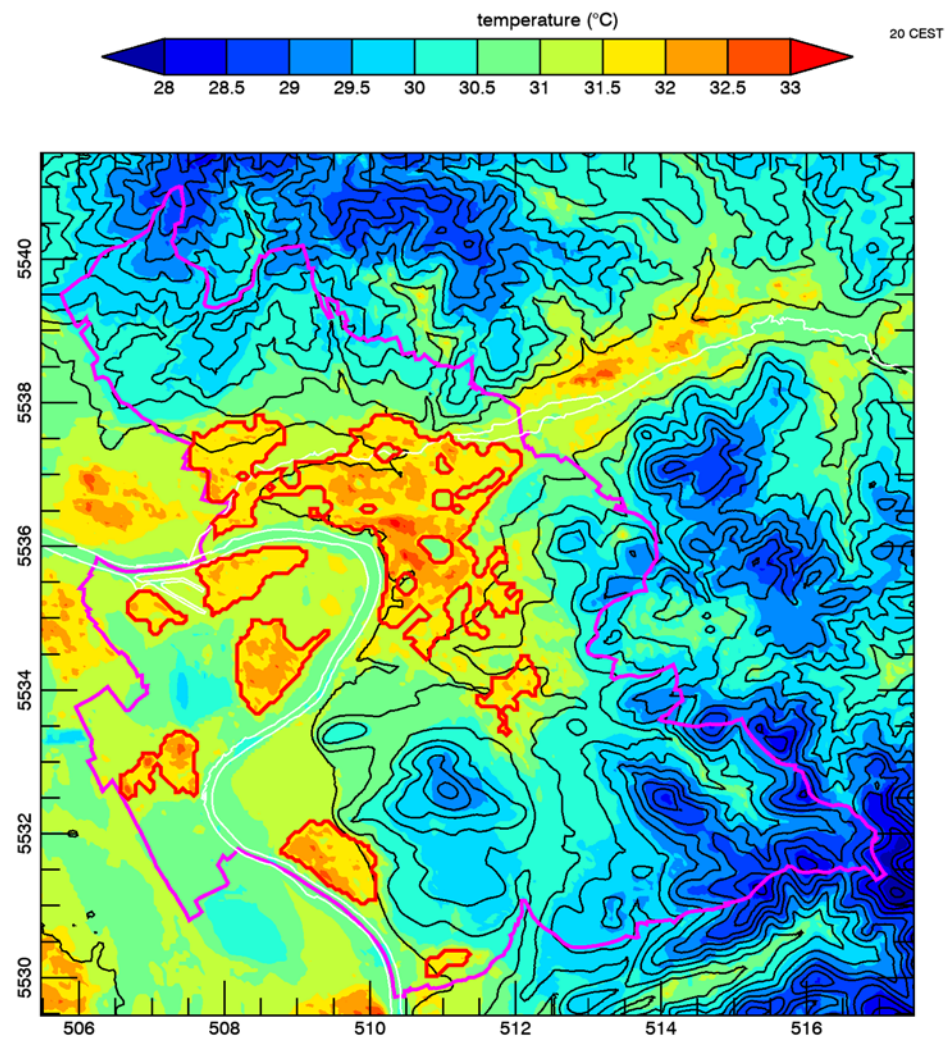
Figure 6. Temperature map (°C) at 5 m above ground level of the 12 km × 12 km city subdomain at 20:00 CEST with thermal hot spots (THs) determined by z-transformation (red contour lines). Terrain elevation contour lines are shown in black, rivers in white and the city border of Aschaffenburg in magenta.

3.2. Delimitated Cold Air Formation Areas (22:00–04:00 CEST)

The CAs delimitation is based on the z-transformation of the integrated sensible heat flux H_{int} from 22:00 until 04:00 CEST in the 12 km × 12 km subdomain of the model area (Figure 7). In built-up areas nocturnal H_{int} values are often positive (heat flux into the atmosphere) due to the release of heat stored in the urban fabric during daytime [1,2]. In rural areas, nocturnal H_{int} values are usually negative. However, the magnitude of their value does not only depend on land cover, but also on the state of the soil and the atmosphere. For example, open spaces (e.g., meadows) in sloping terrain tend to be pronounced CAs, as thermally-driven down-slope winds cause a strong sensible heat flux from the slope wind layer to the surface [9,11]. Therefore, CAs identified by z-transformation in the 12 km × 12 km subdomain are mostly located at slopes around Aschaffenburg (Figure 7).
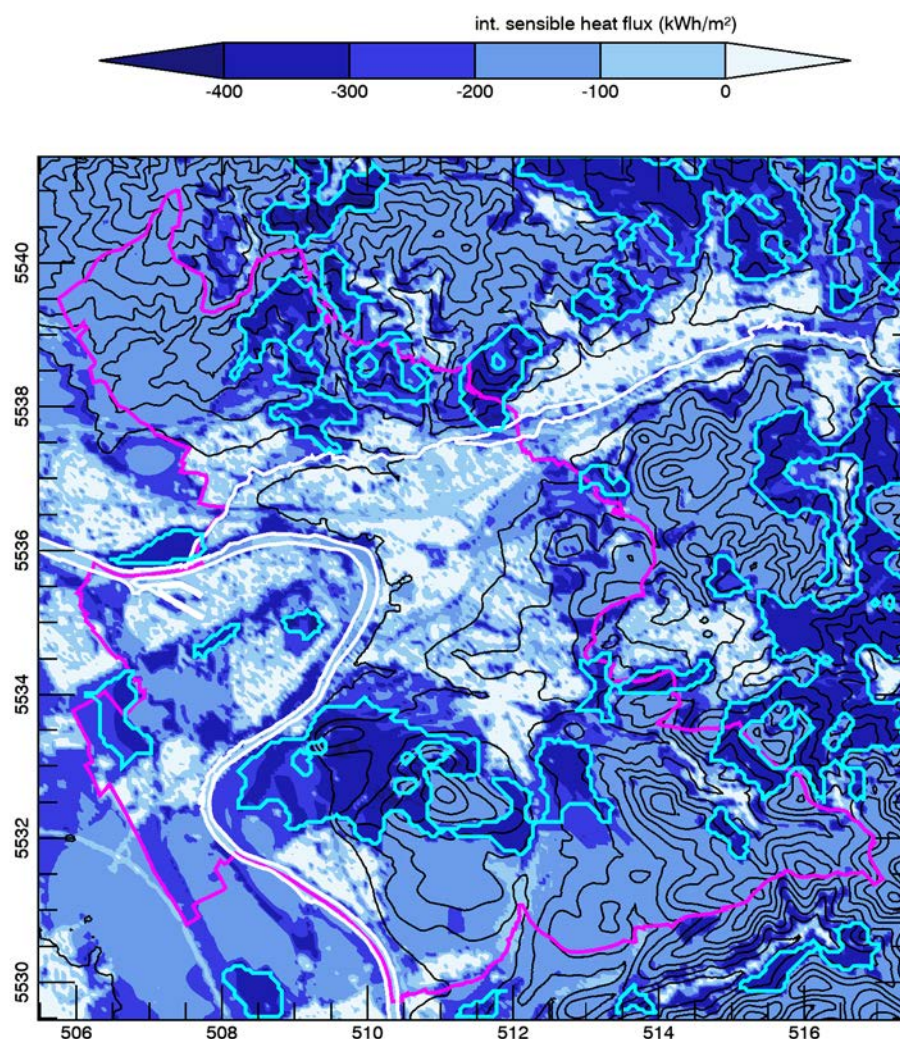
Figure 7. Map of the sensible heat flux (kWh/m^2) between the ground and the atmosphere and between trees and the atmosphere integrated from 22:00 until 04:00 CEST (12 km × 12 km city subdomain). Cold air formation areas (CAs) delimitated by z-transformation are shown in cyan, the terrain elevation contour lines in black, the rivers in white and the city border of Aschaffenburg in magenta.

3.3. Comparison of Land Cover Classes and Delimitation Using z-Transformation on Numerical Model Results

One common way to delimitate either THs or CAs is the usage of land cover, respectively, land cover classes. Based on experience and literature studies, specific land cover classes are directly assigned to local climate features [16,19]. For example, dense building classes are assigned to THs, while pasture and crop classes are assigned to CAs. The effort needed for this approach is low compared to thermodynamic numerical model simulations.

Table 1 shows the frequencies of land cover classes in quantitatively delimitated THs and CAs in relation to the occurrence of the land cover classes in the analysis areas of the objective delimitation (z-transformation). Only 51% of the "pasture" and 59% of the "permanent crops" areas are marked as CAs as not only the physical properties of the model grid cells determine the intensity of nocturnal cold air formation, but also other attributes have a strong influence such as slope inclination, surrounding land cover and atmospheric conditions. Within the municipal boundaries of Aschaffenburg, the majority of model cells with land cover "very dense urban fabric" (93%) and "dense urban fabric" (63%) are identified as TH. It should be noted that some land cover classes such as "permanent crops" are not only represented in the CAs (59%), but in the THs (8%) too. A map showing all

land cover classes and the THs and CAs identified by the z-transformation is presented in the Appendix A (Figure A3).

Table 1. Copernicus Urban Atlas 2012 [41] land cover classes in the model area and their fractions identified as cold air formation areas (CA) and thermal hot spots (TH). Additionally shown is the area the land cover class covers in the 12 km × 12 km domain (CA) and inside the city border of Aschaffenburg (TH). Highlighted in red (land cover THs) and blue (land cover CAs) are the land cover classes used in Figure 8.

No.	Land Cover Class	Land Cover ID	Proportion of CA	Proportion of TH
1	Very dense urban fabric	11100	0.0% of 234 ha	93.0% of 161 ha
3	Dense urban fabric	11210	0.0% of 985 ha	65.2% of 544 ha
4	Medium density urban fabric	11220	0.5% of 480 ha	34.9% of 204 ha
5	Moderate density urban fabric	11230	0.9% of 241 ha	17.0% of 56 ha
6	Low density urban fabric	11240	12.6% of 69 ha	0.0% of 31 ha
7	Isolated Structures	11300	19.6% of 36 ha	0.0% of 16 ha
9	Industrial, commercial, public, military and private units	12100	4.5% of 1252 ha	48.9% 753 ha
10	Highways	12210	1.3% of 94 ha	6.0% of 25 ha
11	Streets and roads	12220	1.8% of 42 ha	33.1% of 31 ha
12	Railways	12230	2.4% of 73 ha	44.6% of 49 ha
13	Port areas	12300	0.0% of 88 ha	51.0% of 88 ha
15	Mineral extraction and dump sites	13100	15.9% of 21 ha	4.3% of 6 ha
16	Construction sites	13300	0.0% of 31 ha	22.4% of 12 ha
17	Unused area	13400	0.0% of 46 ha	11.9% of 30 ha
18	Green urban areas	14100	1.2% of 247 ha	5.2% of 178 ha
19	Sports and leisure facilities	14200	10.8% of 327 ha	7.1% of 222 ha
20	Arable land	21000	37.7% of 1020 ha	0.7% of 220 ha
22	Permanent crops	22000	58.7% of 30 ha	8.1% of 28 ha
23	Pastures	23000	51.3% of 3957 ha	1.3% of 1400 ha
27	Forest	31000	3.6% of 4884 ha	0.0% of 2146 ha
31	Herbaceous vegetation associations	32000	32.1% of 21 ha	0.0% of 2 ha
33	Water	50000	0.0% of 223 ha	0.3% of 172 ha

In order to illustrate the differences between the land cover approach and the quantitative delimitation, an example is shown in Figure 8. For the comparison in Figure 8, all land cover classes ≥14% mean building surface fraction are used for land cover based THs (class numbers 1, 3, 4, 5, 9 and 13 indicated in red font in Table 1), and the four rural land cover classes for open spaces without buildings are used for land cover based CAs (class numbers 20, 22, 23 and 31, indicated in blue font in Table 1). While the total areas of THs and CAs delimitated by z-transformation are 1086 hectares and 2740 hectares, respectively, the land cover approach identifies 1805 hectares for THs and 5028 hectares for CAs. This indicates that a direct linkage between land cover and THs or cold air formation in complex terrain is a highly simplified approach. CAs identified over sloping terrain reveal good agreement between the two approaches. However, the land cover approach overestimates the existence of CAs in the Main Valley and of THs in the southeastern suburbs of Aschaffenburg. Overall, the land cover approach can still be useful if no spatial coverage of climate data is available, but applications for urban or regional planning have to take the limitations of this method into account.
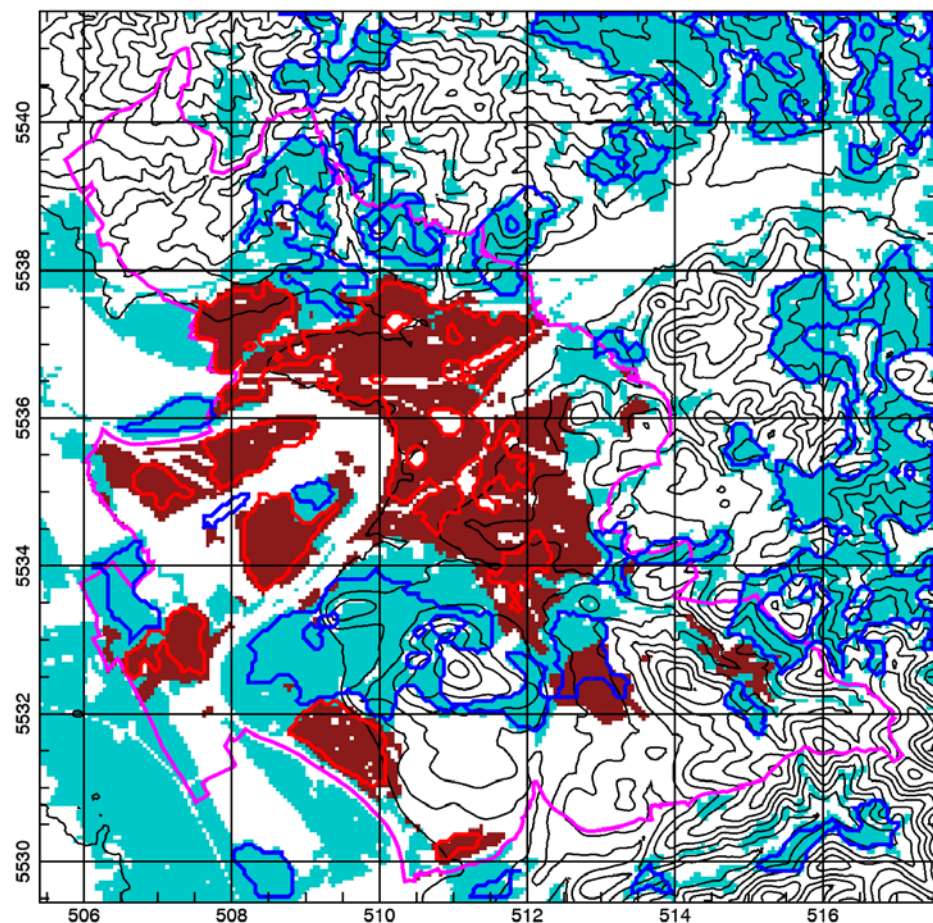
Figure 8. Map of thermal hot spots (THs, dark red areas) and cold air formation areas (CAs, cyan areas) from the land cover approach compared to the quantitative delimitation of THs (red outline) and of CAs (blue outline) in the 12 km × 12 km subdomain. Additionally, the city border of Aschaffenburg is shown as a magenta line and the terrain elevation in black contour lines.

3.4. Trajectory Analysis

3.4.1. Nocturnal Backward Trajectories (01:00–23:00 CEST, 03:00–01:00 CEST)

Figure 9 illustrates the backward trajectories with their origin in the TH polygons at 01:00 CEST, calculated backwards in time until 23:00 CEST. These trajectories indicate where the air arriving in THs at 01:00 CEST are starting at 23:00 CEST and which path the air took on its way towards THs. TRACA sets the starting point of the trajectories randomly in the TH polygons. Due to varying building heights in THs, trajectories are chosen to start randomly between 5 m and 15 m agl. Green color shading of the trajectories indicates their height above ground level.

Due to effects of country breezes (see Figure 4), trajectories show pronounced flow convergences, particularly in the city center and in western suburbs close to the Main River. Air flowing along trajectories originating in, or passing over CAs at low heights, will experience cooling, while trajectory paths crossing settlements (in particular THs) at low elevations are prone to warming and are possibly exposed to emissions of air pollutants. Nocturnal cooling of the air over slopes is mostly limited to heights below 50 m agl, trajectories above 50 m agl are therefore not considered relevant for nocturnal cooling in urban quarters. Since some trajectories in Figure 9 rise to heights above 50 m agl (for example along the Aschaff Valley), the calculation of trajectories for Aschaffenburg has been limited to 2 h.

Figure 9 shows that early in the night not all objectively delimited CAs are (equally) important for the ventilation of Aschaffenburg. Most eastern CAs (located in side valleys in

the upper Aschaff Valley) are not connected to the city by backward trajectories. However, most northern and southern CAs are directly linked to the TH polygons in the city and are therefore elementary for its nocturnal cooling and ventilation.
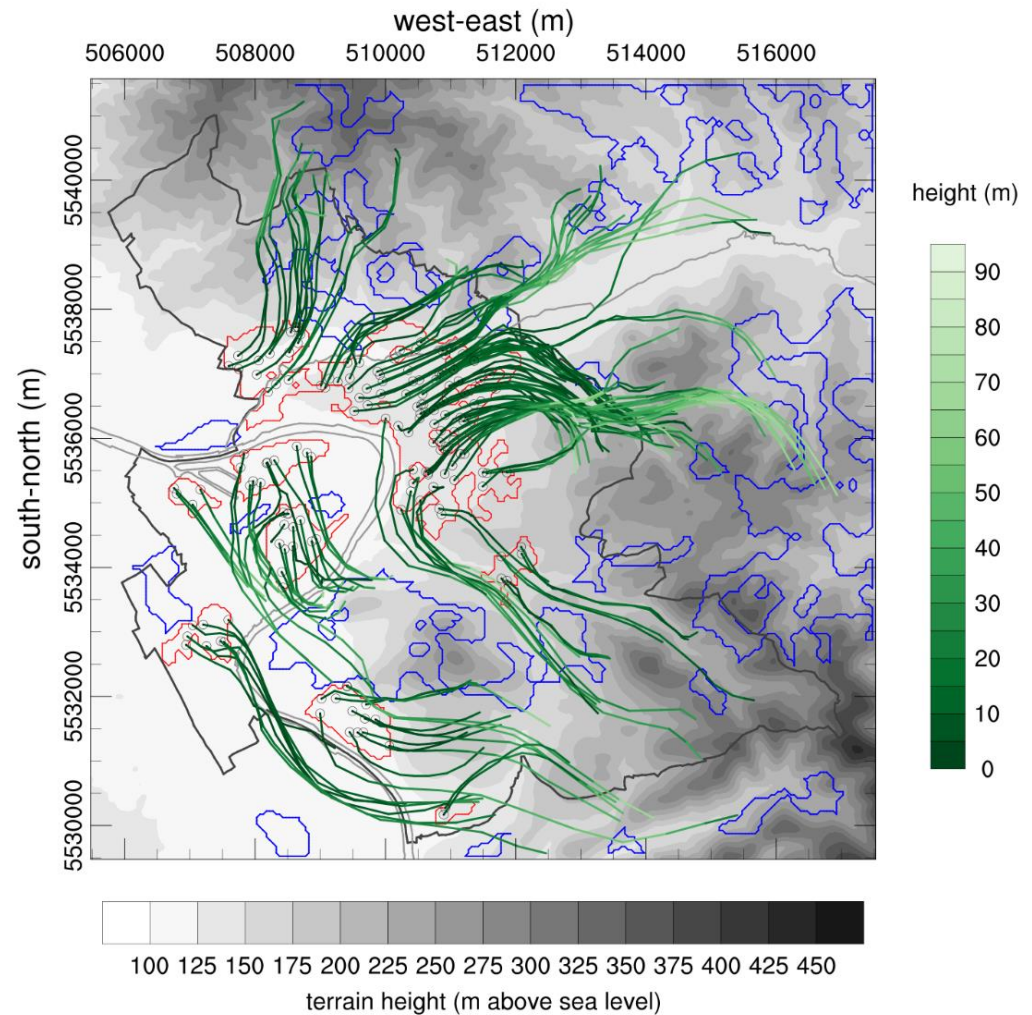

Figure 9. Backward trajectory map of the 12 km × 12 km subdomain from 01:00 to 23:00 CEST with trajectory heights above ground level in green color shading. Trajectories are released in the thermal hot spots (red contour) identified by z-transformation. Additionally shown are the cold air formation areas in blue, rivers in light grey, the city border of Aschaffenburg in black lines and terrain elevation in grey color shading.

Backward trajectories calculated later in the night from 03:00 to 01:00 CEST are influenced by changes in the simulated wind field (Figure 10). Due to the weakening urban heat island intensity, the forcing of country breezes decreases and the northeasterly down-valley winds in the Aschaff Valley become clearly more dominant. Due to the changes in wind speed and direction of drainage winds, the connectivity of some surrounding CAs with THs in Aschaffenburg is now more established (Figure 10). However, there are no CAs along the floor of the Aschaff Valley (Figure 7), as the valley floor is mostly covered by industrial areas and settlements (see Figures 2b and 3). The intensified down-valley winds in the Aschaff Valley enhances the along-valley air exchange rates, but the air arriving in Aschaffenburg is characterized by a small temperature deficit and impacted by anthropogenic emissions.
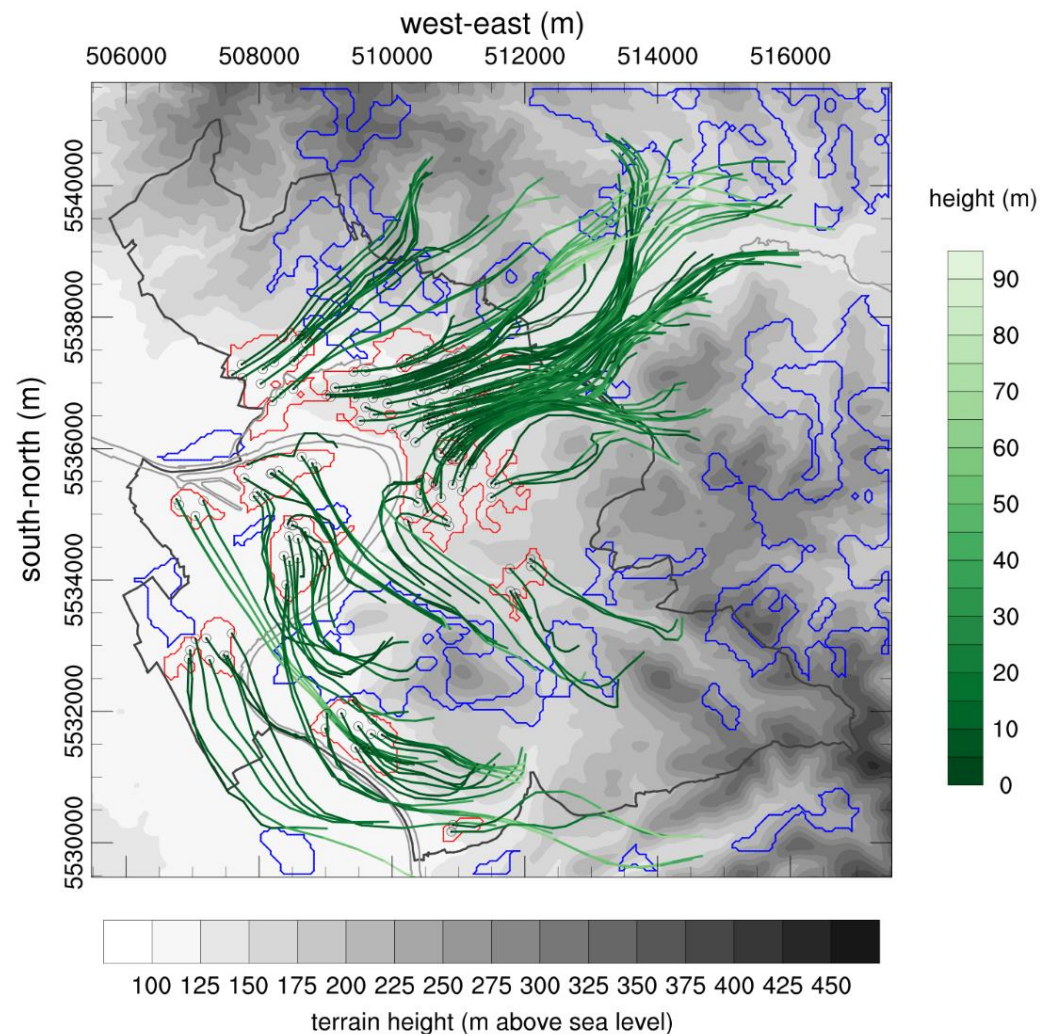
Figure 10. Backward trajectory map of the 12 km × 12 km subdomain from 03:00 to 01:00 CEST with trajectory heights above ground level in green color shading. Trajectories are released in the thermal hot spots (red) identified by z-transformation. Additionally shown are the cold air formation areas in blue, rivers in light grey, the city border of Aschaffenburg in black and terrain elevation in grey color shading.

3.4.2. Nocturnal Forward Trajectories (23:00–01:00 CEST, 01:00–03:00 CEST)

Calculations of forward trajectories are a complementary way to determine which CAs are relevant for nocturnal ventilation in Aschaffenburg, in particular regarding CAs for which no connection to THs was found from backward trajectories. To ensure their cool origin, forward trajectories are started in CAs at the fixed height of 5 m agl. Figure 11 shows forward trajectories calculated early in the night from 23:00 to 01:00 CEST. The forward trajectories from CAs around the city center reach multiple THs and reveal similar airflow patterns as backward trajectories from THs for the same time interval (Figure 9). However, Figure 11 also reveals that nocturnal cold air forming further away in tributaries of the upper Aschaff Valley (northeastern CAs) drains into the Aschaff Valley. Within two hours of integration the air reaches the fringe of the TH in the city center, partly at high elevations and therefore of limited relevance for cooling Aschaffenburg. Some cold air forming in eastern CAs also reaches the southern fringe of the TH in the city center at elevated heights from a southeasterly direction.
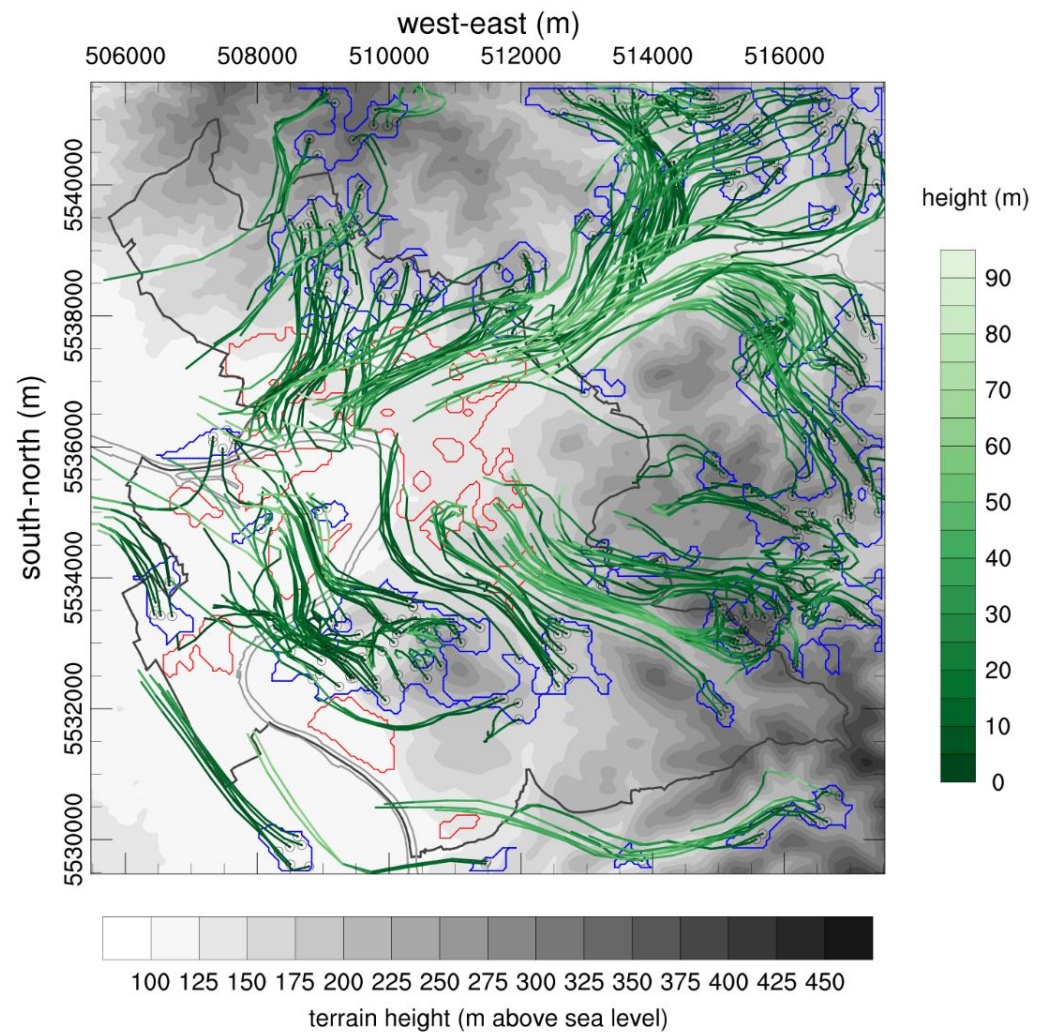
Figure 11. Forward trajectory map of the 12 km × 12 km subdomain from 23:00 to 01:00 CEST with trajectory heights above ground level in green color shading. Trajectories are released in the cold air formation areas (blue) identified by z-transformation. Additionally shown are the thermal hot spots in red, rivers in light grey, the city border of Aschaffenburg in black and terrain elevation in grey color shading.

Forward trajectories calculated later in the night from 01:00 to 03:00 CEST (Figure 12) show a stronger alignment of the wind field along the Aschaff Valley similar to the backward trajectories (Figure 10). The more pronounced down-valley winds block cold airflow originating in some central eastern CAs from entering the Aschaff Valley and therefore from reaching THs in Aschaffenburg. The air from the northeastern CAs still reaches Aschaffenburg several decameters above ground and its cooling function for Aschaffenburg is therefore limited. As already found earlier in the night, drainage winds from CAs located on slopes north and south of the city remain the most important for cooling THs in Aschaffenburg.
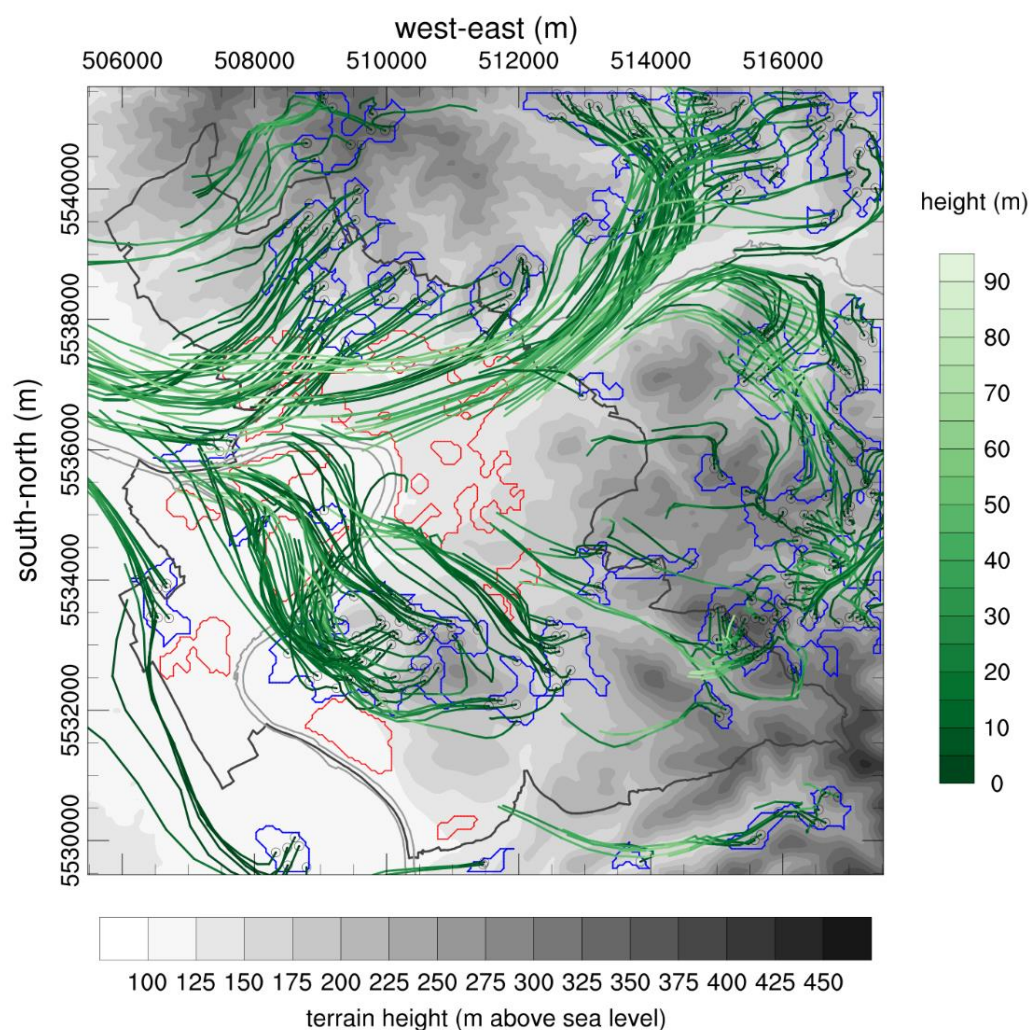
Figure 12. Forward trajectories map of the 12 km × 12 km subdomain from 01:00 to 03:00 CEST with trajectory heights above ground level in green color shading. Trajectories are released in the cold air formation areas (blue) identified by z-transformation. Additionally shown are the thermal hot spots in red, rivers in light grey, the city border of Aschaffenburg in black and terrain elevation in grey color shading.

4. Discussion and Conclusions

Climate resilient urban planning requires information on city locations which are particularly affected by strong heat load and how the local winds can provide cooling to these quarters, particularly during nighttime when UHI intensities are highest. Source areas of strong cold air formation generating these local winds need to be protected and ventilation paths, along which local winds reach heat prone quarters, have to be preserved as building and emission restriction zones. In this study the results from the numerical urban climate model MUKLIMO_3 for an idealized calm and clear summertime weather situation with 50 m horizontal grid spacing are used to identify thermal hotspots (THs) in the medium-sized town of Aschaffenburg and to locate strong cold air formation areas (CAs) in the hilly airshed around the city.

THs and CAs are identified using the z-transformation for statistical normalization of smoothed near surface air temperature and time-integrated sensible heat fluxes. The applicability of the obtained THs and CAs for urban ventilation studies is demonstrated using the post-processing tool TRACA to calculate backward trajectories from THs and forward trajectories from CAs for two periods during nighttime.

4.1. Main Findings

The main findings of the presented approach are:

- The applied z-transformation is suitable for the quantitative identification of the most pronounced areas of cold air formation in the rural surrounding of the city and of hot spots within the built-up urban quarters
- Spatial smoothing of the numerical model results in combination with a minimum area size of 125,000 m^2 for THs and CAs allows the identification of relevant areas for urban and landscape planning
- Backward trajectories show which THs receive venting from CAs or other areas inside or outside the city
- Forward trajectories imply that cold air from the CAs in the nearby hilly surroundings reach the THs in the city. However, airflow originating in some CAs (e.g., located in the upper Main Valley or further away in the mountains) either does not reach THs in Aschaffenburg, or they are less relevant as airflow detaches from the surface prior to its arrival at THs
- Statistical analysis of land cover types in delimitated THs and CAs reveal that the application of z-transformation to numerical urban climate model results provides a more sophisticated picture of urban climate functions than the traditional approach of climatopes. This is mainly due to the fact that numerical urban climate models consider dynamic feedbacks between surface energy exchanges and atmospheric mixing

In conclusion, the presented approach provides guidance to urban planners on which city districts are particularly exposed to heat stress and which crucial areas must be preserved for nocturnal cold air formation. The presented airflow trajectory analysis shows that wind-induced transport of cool air from CAs is not bound to municipal boundaries. On the one hand, Aschaffenburg benefits from cool air forming in neighboring communities, and on the other hand, municipalities located downwind benefit from some CAs in Aschaffenburg, which are not relevant for the ventilation of THs in Aschaffenburg. Climate resilient urban planning therefore requires expedient cooperation with neighboring communities as well as on the regional scale.

4.2. Limitations and Outlook

Results of area delimitation using z-transformation strongly depend on the spatial variability and spread of the analyzed variable and hence on the variability of terrain height and land cover. Therefore, most obviously, delimitation results are influenced by the choice of the analyzed domain, but also on data filtering prior to z-transformation. In this study, TH detection has been limited to grid cells within the municipal boundaries of Aschaffenburg, with most built-up areas being located at similar elevations on the valley floor. Therefore, it is no surprise that hot spots were identified in areas with high and dense buildings. However, the approach of this study may reach its limit when other factors influencing the air temperature are stronger than building effects. For a city located on a slope or hilltop with great terrain elevation differences within the municipality, z-transformation could possibly identify THs in grid cells with very low terrain elevation although these grid cells may have rural land cover and do not represent the hottest areas in the city. A possible solution would be to divide the study area into elevation classes to eliminate the effect of orography on the temperature signal or to reduce elevation effects by analyzing potential temperature instead of air temperature.

In this study the delimitation of pronounced CAs is performed for a domain of 12 km × 12 km covering most of the Aschaff Valley airshed, but z-transformation was limited to grid cells having negative values of time-integrated sensible heat flux. Most CAs are identified in open spaces on slopes, e.g., with land cover being pasture or crops. Future research could therefore investigate objective TH and CA delimitation for cities located on slopes, hill tops or more variable relief in general, and for cities located near a lake or coast. The study could also be extended by analyzing additional urban climate simulations, e.g., for situations with different regional wind directions.

Unfortunately, detailed climate measurements for validating simulated wind and air temperature variability within and around Aschaffenburg are not available. However, good agreement between simulation results and observations were found in previous studies using the urban climate model MUKLIMO_3 [9,38,45]. It should also be noted that there is still a paucity of studies on the nocturnal cooling potential of forested areas and on the capability of computer models to simulate forest climate correctly [45–48]. The drainage wind airshed of Aschaffenburg is covered by extended forest areas, which have not been identified as strong CAs as the magnitude of the time-integrated sensible heat flux H_{int} is about 50% lower than H_{int} values in open spaces on sloping terrain (Figure 7). However, areas with only moderate cooling potential could still be very relevant for urban planning, if such areas are extended enough and the generated cold airflow is directed towards urban hot spots. Future studies should develop methods for objective delimitation of relevant CAs that combine information on the magnitude of local cold air formation with the spatial extension of CAs.

Conflicts of Interest: The authors declare no conflict of interest.

Appendix A

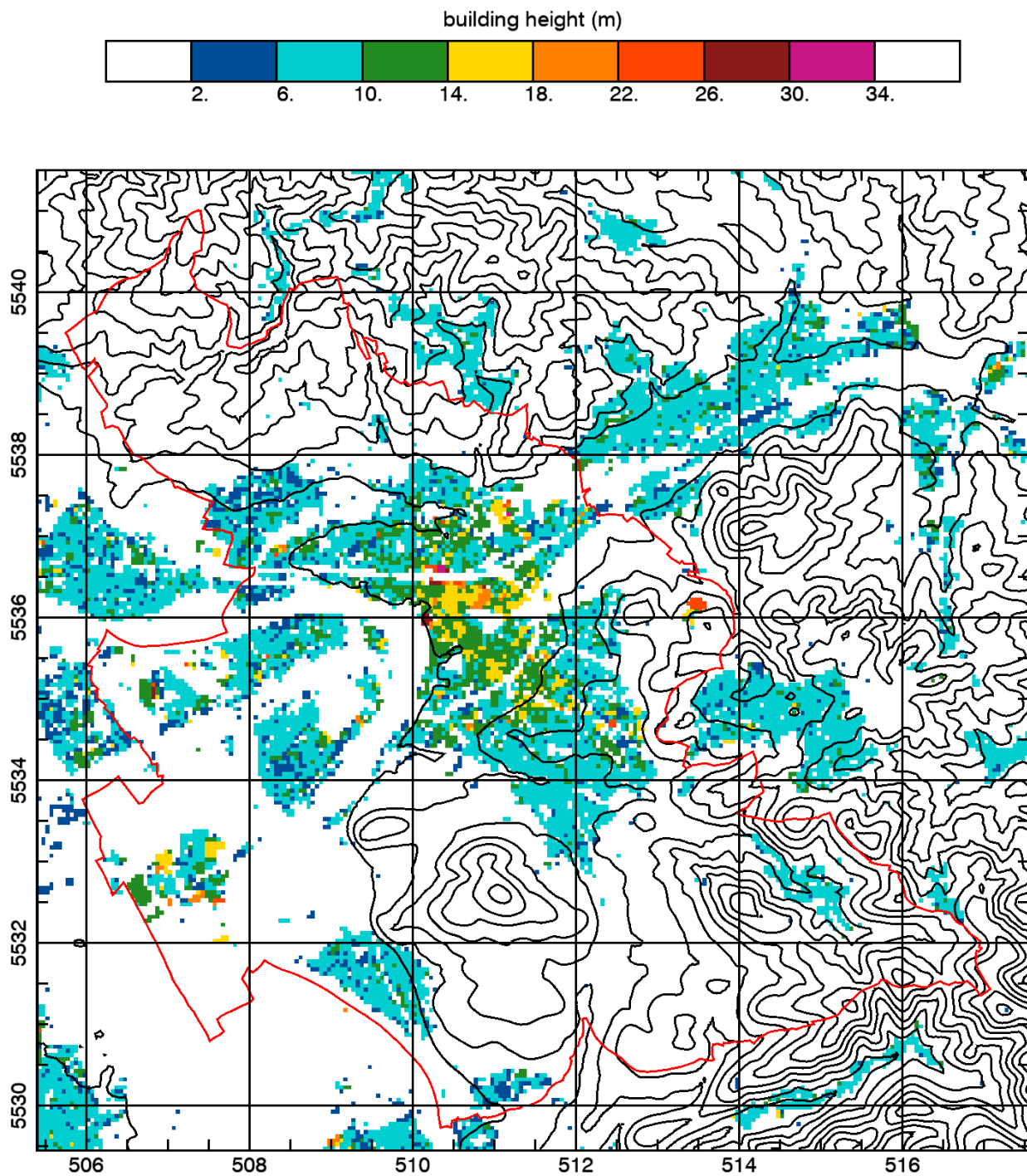**Figure A1.** Map of building height in the 12 km × 12 km city subdomain, the terrain elevation contour lines in black and the city border of Aschaffenburg in red [30].
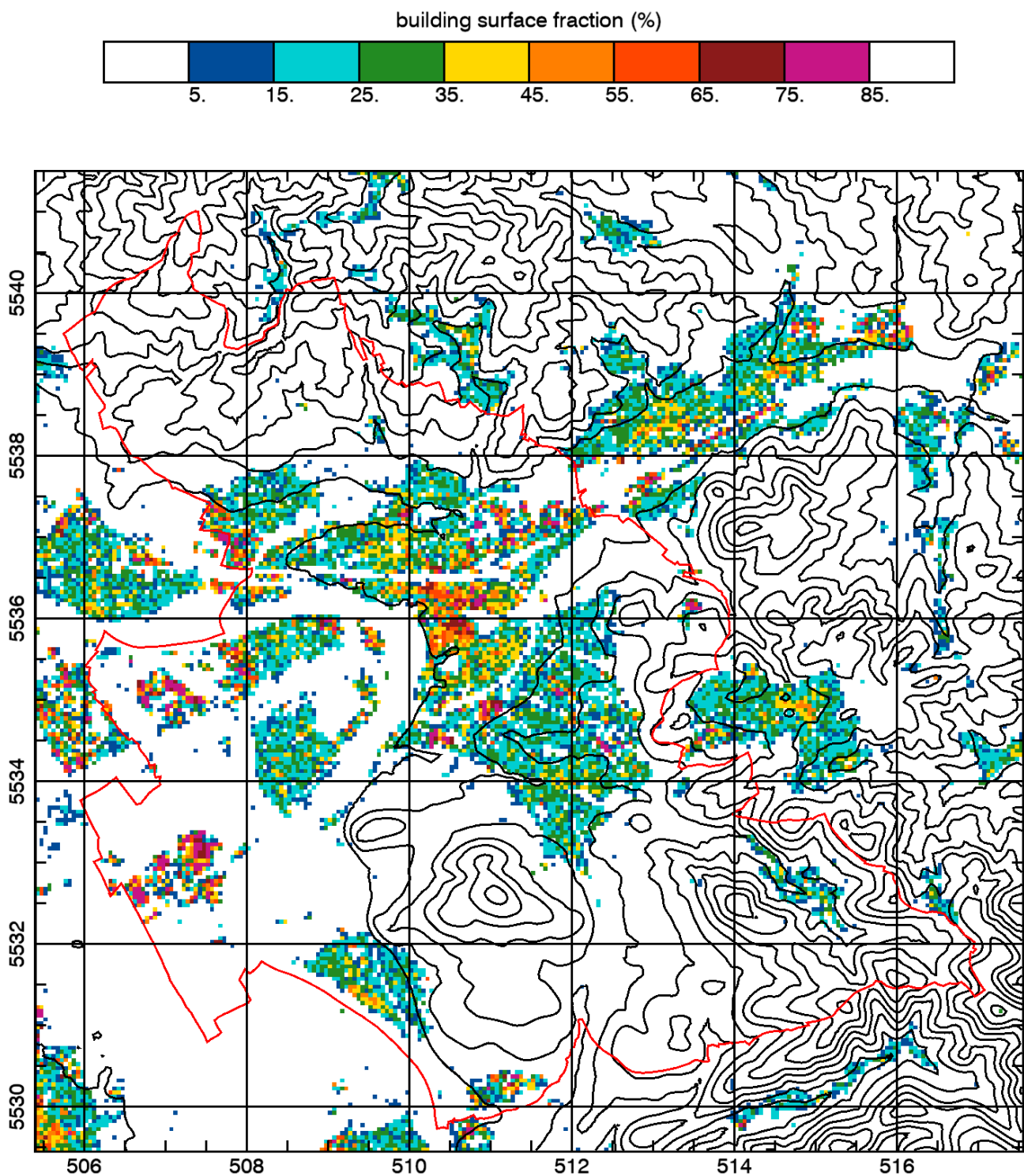
Figure A2. Map of the building surface fraction in the 12 km × 12 km city subdomain, the terrain elevation contour lines in black and the city border of Aschaffenburg in red [30].
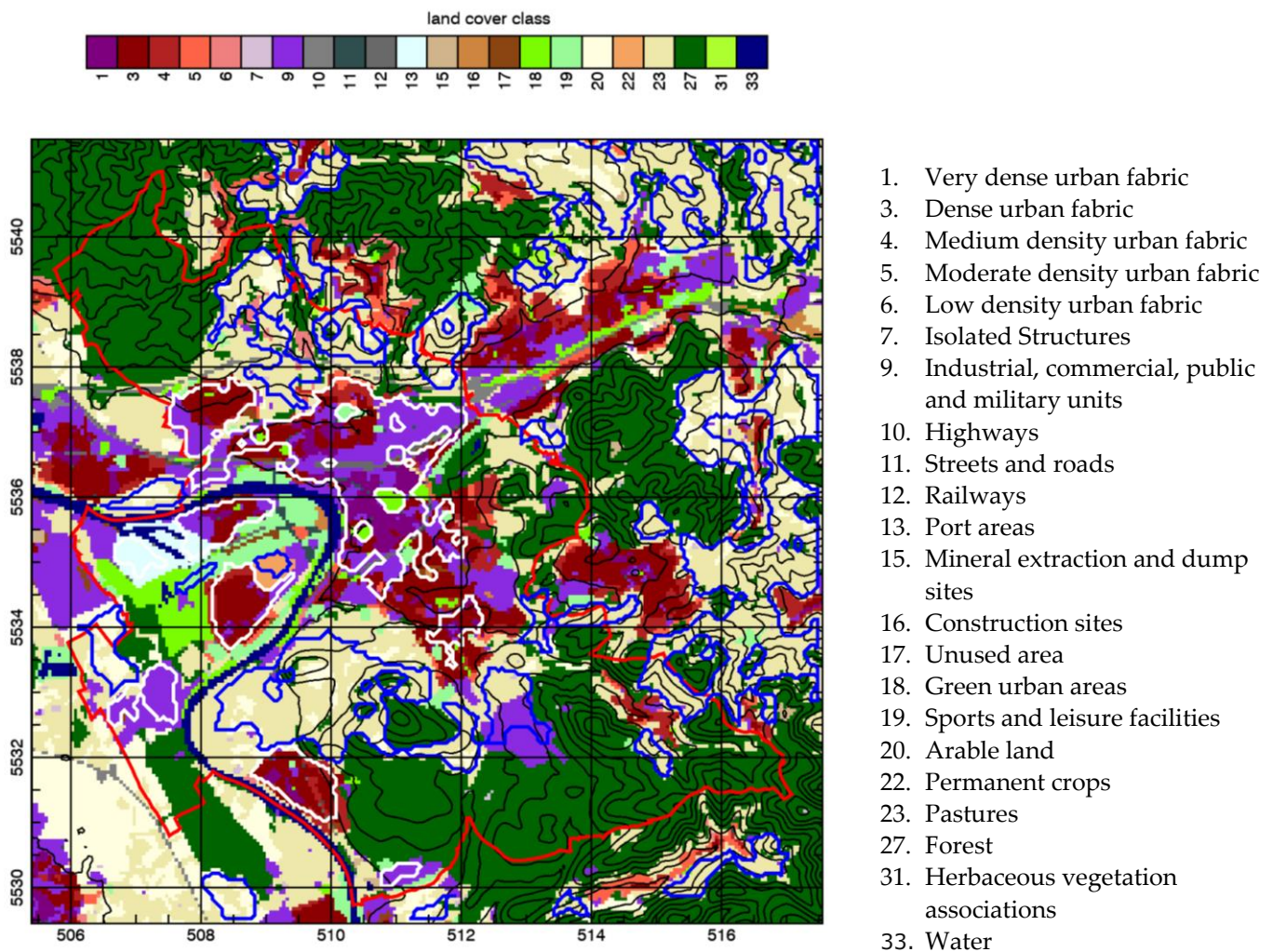
Figure A3. Land cover classification map in the 12 km × 12 km subdomain (Figure 2a) with the city border of Aschaffenburg (red), quantitatively delimited thermal hot spots (white) and cold air formation areas (blue). Black contour lines represent terrain elevation in 25 m height intervals.

1. Very dense urban fabric
3. Dense urban fabric
4. Medium density urban fabric
5. Moderate density urban fabric
6. Low density urban fabric
7. Isolated Structures
9. Industrial, commercial, public and military units
10. Highways
11. Streets and roads
12. Railways
13. Port areas
15. Mineral extraction and dump sites
16. Construction sites
17. Unused area
18. Green urban areas
19. Sports and leisure facilities
20. Arable land
22. Permanent crops
23. Pastures
27. Forest
31. Herbaceous vegetation associations
33. Water

References

1. Oke, T.R.; Mills, G.; Christen, A.; Voogt, J.A. *Urban Climates*; Cambridge University Press: Cambridge, UK, 2017.
2. Stewart, I.D.; Mills, G. *The Urban Heat Island: A Guide Book*; Elsevier: Amsterdam, The Netherlands, 2021.
3. IPCC. Summary for Policymakers. In *Climate Change 2021: The Physical Science Basis. Contribution of Working Group I to the Sixth Assessment Report of the Intergovernmental Panel on Climate Change*; Masson-Delmotte, V., Zhai, P., Pirani, A., Connors, S.L., Péan, C., Berger, S., Caud, N., Chen, Y., Goldfarb, L., Gomis, M.I., et al., Eds.; Cambridge University Press: Cambridge, UK; New York, NY, USA, 2021; pp. 3–32. [CrossRef]
4. Barlag, A.-B.; Kuttler, W. The significance of country breezes for urban planning. *Energy Build.* **1990–1991**, *15*, 291–297. [CrossRef]
5. Haeger-Eugensson, M.; Holmer, B. Advection caused by the urban heat island circulation as a regulating factor on the nocturnal urban heat island. *Int. J. Climatol.* **1999**, *19*, 975–988. [CrossRef]
6. Gross, G. On the self-ventilation of an urban heat island. *Meteorol. Z.* **2019**, *28*, 87–92. [CrossRef]
7. Gross, G. Numerical simulation of the nocturnal flow systems in the Freiburg area for different topographies. *Contr. Atmos. Phys.* **1989**, *62*, 57–72.
8. Fernando, H.J.S. Fluid dynamics of urban atmospheres in complex terrains. *Annu. Rev. Fluid Mech.* **2010**, *42*, 365–389. [CrossRef]
9. Schau-Noppel, H.; Kossmann, M.; Buchholz, S. Meteorological information for climate-proof urban planning—The example of KLIMPRAX. *Urban Clim.* **2020**, *32*, 100614. [CrossRef]
10. Whiteman, C.D. *Mountain Meteorology: Fundamentals and Applications*; Oxford University Press: Oxford, NY, USA, 2000.
11. Zardi, D.; Whiteman, C.D. Diurnal Mountain Wind Systems. In *Mountain Weather Research and Forecasting: Recent Progress and Current Challenges*; Chow, F.K., De Wekker, S.F.J., Snyder, B.J., Eds.; Springer: Dordrecht, The Netherlands, 2013; pp. 11–35.
12. Masson, V.; Lion, Y.; Peter, A.; Pigeon, G.; Buyck, J.; Brun, E. "Grand Paris": Regional landscape change to adapt city to climate warming. *Clim. Chang.* **2013**, *117*, 769–782. [CrossRef]

13. Ren, C.; Yang, R.; Cheng, C.; Xing, P.; Fang, X.; Zhang, S.; Wang, H.; Shi, Y.; Zhang, X.; Kwok, Y.T.; et al. Creating breathing cities by adopting urban ventilation assessment and wind corridor plan—The implementation in Chinese cities. *J. Wind Eng. Industr. Aerodyn.* **2018**, *182*, 170–188. [CrossRef]

14. Grunwald, L.; Kossmann, M.; Weber, S. Mapping urban cold-air paths in a Central European city using numerical modelling and geospatial analysis. *Urban Clim.* **2019**, *29*, 100503. [CrossRef]

15. Lazar, R.; Podesser, A. An urban climate analysis of Graz and its significance for urban planning in the tributary valleys east of Graz (Austria). *Atmos. Environ.* **1999**, *33*, 4195–4209. [CrossRef]

16. Ren, C.; Ng, E.Y.; Katzschner, L. Urban climatic map studies: A review. *Int. J. Climatol.* **2011**, *31*, 2213–2233. [CrossRef]

17. Sturman, A.; Zawar-Reza, P. Application of back-trajectory techniques to the delimitation of urban clean air zones. *Atmos. Environ.* **2002**, *36*, 3339–3350. [CrossRef]

18. Xu, Y.; Wang, W.; Chen, B.; Chang, M.; Wang, X. Identification of ventilation corridors using backward trajectory simulations in Beijing. *Sustain. Cities Soc.* **2021**, *70*, 102889. [CrossRef]

19. VDI. *Climate and Air Pollution Maps for Cities and Regions*; Verein Deutscher Ingenieure, Guideline 3787/1; Beuth Verlag GmbH: Berlin, Germany, 2015.

20. Reuter, U.; Kapp, R. *Climate Booklet for Urban Development—Indications for Urban Land-Use Planning*; Ministry of Economy, Work and Housing of Baden: Württemberg, Germany, 2012; Available online: https://www.staedtebauliche-klimafibel.de/ (accessed on 8 July 2022).

21. Scherer, D.; Fehrenbach, U.; Beha, H.-D.; Parlow, E. Improved concepts and methods in analysis and evaluation of the urban climate for optimizing urban planning processes. *Atmos. Environ.* **1999**, *33*, 4185–4193. [CrossRef]

22. Moriyama, M.; Takebayashi, H. Making method of "Klimatope" map based on normalized vegetation index and one-dimensional heat budget model. *J. Wind Eng. Industr. Aerod.* **1999**, *81*, 211–220. [CrossRef]

23. Fehrenbach, U.; Scherer, D.; Parlow, E. Automated classification of planning objectives for the consideration of climate and air quality in urban and regional planning for the example of the region of Basel/Switzerland. *Atmos. Environ.* **2001**, *35*, 5605–5615. [CrossRef]

24. Stewart, I.D.; Oke, T.R. 'Local climate zones' for urban temperature studies. *Bull. Am. Meteorol. Soc.* **2012**, *93*, 1879–1900. [CrossRef]

25. Demuzere, M.; Kittner, J.; Martilli, A.; Mills, G.; Moede, C.; Stewart, I.D.; van Vliet, J.; Bechtel, B. A global map of Local Climate Zones to support earth system modelling and urban scale environmental science. *Earth Syst. Sci. Data Discuss.* 2022; *in review*. Available online: https://essd.copernicus.org/preprints/essd-2022-92/(accessed on 8 July 2022).

26. Stewart, I.D.; Oke, T.R.; Krayenhoff, E.S. Evaluation of the 'local climate zones' scheme using temperature observations and model simulations. *Int. J. Climatol.* **2013**, *34*, 1062–1080. [CrossRef]

27. VDI. *Methods and Presentation of Investigations Relevant for Planning Urban Climate*; Verein Deutscher Ingenieure, Guideline 3785/1; Beuth Verlag GmbH: Berlin, Germany, 2008.

28. Deutscher Wetterdienst. CDC (Climate Data Center). Available online: www.dwd.de/cdc (accessed on 2 May 2022).

29. Deutscher Wetterdienst. German Climate Atlas. Available online: www.dwd.de/klimaatlas (accessed on 2 May 2022).

30. BKG. Aktualisiertes 3D-Gebäudemodell im Level of Detail 1. Bundesamt für Kartographie und Geodäsie [German Federal Agency for Cartography and Geodesy]. 2019. Available online: https://www.bkg.bund.de/SharedDocs/Produktinformationen/BKG/DE/P-2019/190211_LoD1.html (accessed on 2 May 2022).

31. Sievers, U.; Zdunkowski, W. A microscale urban climate model. *Contr. Atmos. Phys.* **1985**, *59*, 13–40.

32. Sievers, U. Generalization of the stream-function method to three dimensions. *Meteorol. Z.* **1995**, *4*, 3–15. [CrossRef]

33. Sievers, U.; Forkel, R.; Zdunkowski, W. Transport equations for heat and moisture in the soil and their application to boundary layer problems. *Contr. Atmos. Phys.* **1983**, *56*, 58–83.

34. Möller, F. Ein Kurzverfahren zur Bestimmung der langwelligen Ausstrahlung dicker Atmosphärenschichten. *Archiv für Meteorologie Geophysik und Bioklimatologie Serie A* **1953**, *7*, 158–169. [CrossRef]

35. Sievers, U.; Früh, B. A practical approach to compute short-wave irradiance interacting with subgrid-scale buildings. *Meteorol. Z.* **2012**, *21*, 349–364. [CrossRef]

36. Siebert, J.; Sievers, U.; Zdunkowski, W. A one-dimensional simulation of the interaction between land surface processes and the atmosphere. *Boundary-Layer Meteorol.* **1992**, *59*, 1–34. [CrossRef]

37. Bokwa, A.; Dobrovoly, P.; Gal, T.; Geletic, J.; Gulyas, A.; Hajto, M.J.; Holec, J.; Hollosi, B.; Lehnert, M.; Sarbit, N.; et al. Urban climate in Central European cities and global climate change. *Acta Clim.* **2018**, *51–52*, 7–35. [CrossRef]

38. Geletic, J.; Lehnert, M.; Dobrovolny, P.; Zuvela-Aloise, M. Spatial modelling of summer climate indices based on local climate zones: Expected changes in the furture climate of Brno, Czech Republic. *Clim. Chang.* **2019**, *152*, 487–502. [CrossRef]

39. Gal, T.; Maho, S.I.; Skarbit, N.; Unger, J. Numerical modelling for analysis of the effect of different urban green spaces on urban heat load patterns in the present and in the future. *Comput. Environ. Urban Syst.* **2021**, *87*, 101600. [CrossRef]

40. Hollosi, B.; Zuvela-Aloise, M.; Oswald, S.; Kainz, A.; Schöner, W. Applying urban climate model in prediction mode—Evaluation of MUKLIMO_3 model performance for Austrian cities based on the summer period of 2019. *Theor. Appl. Climatol.* **2021**, *144*, 1181–1204. [CrossRef]

41. European Environment Agency. Urban Atlas. 2012. Available online: https://land.copernicus.eu/local/urban-atlas/urban-atlas-2012 (accessed on 2 May 2022).

42. European Environment Agency. High Resolution Layers. 2012. Available online: https://land.copernicus.eu/pan-european/high-resolution-layers (accessed on 2 May 2022).
43. BKG. Digital Topographic Map DTK 1:200000, Bundesamt für Kartographie und Geodäsie [German Federal Agency for Cartography and Geodesy]. 2020. Available online: https://daten.gdz.bkg.bund.de/produkte/dtk/dtk200-v/2015/dtk200-v_eng.pdf (accessed on 17 May 2022).
44. Keck, M. *TRACA Manual. Technical Instructions for Installation and Application*; Institute of Meteorology and Climatology: Hannover, Germany, 2014.
45. Straka, M.; Sodoudi, S. Evaluating climate change adaptation strategies and scenarios of enhanced vertical and horizontal compactness at urban scale (a case study for Berlin). *Landsc. Urban Plan.* **2019**, *183*, 68–78. [CrossRef]
46. Kiefer, M.T.; Zhong, S. The effect of sidewall forest canopies on the formation of cold-air pools: A numerical study. *J. Geophys. Res. Atmos.* **2013**, *118*, 5965–5978. [CrossRef]
47. Kiefer, M.T.; Zhong, S. The role of forest cover and valley geometry in cold-air pool evolution. *J. Geophys. Res. Atmos.* **2015**, *120*, 8693–8711. [CrossRef]
48. De Wekker, S.F.J.; Kossmann, M.; Knievel, J.C.; Giovannini, L.; Gutmann, E.; Zardi, D. Meteorological applications benefiting from an improved understanding of atmospheric exchange processes over mountains. *Atmosphere* **2018**, *9*, 371. [CrossRef]